

# Molecular Weight Dependence of Nuclear Spin Correlations in PDMS Networks

P. T. Callaghan<sup>†</sup> and E. T. Samulski<sup>\*‡</sup>

Department of Physics, Massey University, Palmerston North, New Zealand, and Department of Chemistry, University of North Carolina at Chapel Hill, Chapel Hill, North Carolina 27599-3290

Received January 4, 2000; Revised Manuscript Received February 28, 2000

**ABSTRACT:** We present experimental proton NMR data for poly(dimethylsiloxane) (PDMS) model networks in the form of a  $\beta$ -echo (sine correlation) function which is particularly sensitive to modulations of nuclear dipolar interactions caused by slow molecular reorientations. The  $\beta$ -echo can be computed with a correlation function which allows for preaveraging of local dipolar interactions—methyl group rotation, intra-Kuhn-segment isomerization, extra-segment reorientations due to (restricted) Rouse modes, and slower modulations due to network fluctuations—to yield a residual proton second moment,  $\overline{M}_2$ . The data were obtained from networks with inter-cross-link molar mass,  $M_x$ , covering a wide range both below and above the entanglement mass,  $M_e$ . Fits of the  $\beta$ -echo give quite reliable estimates of the preaveraged dipolar interaction strength  $\overline{M}_2$ , and these indicate a clear dependence on  $M_x$ , in which the role of physical entanglements is dramatically evident. Network dynamics cannot be reliably ascertained due to the effect of higher-order spin interactions.

## Introduction

The elasticity of a polymeric rubber above its glass transition temperature is an intriguing manifestation of cooperative macromolecular statics and dynamics. It derives from entropic considerations when the topology of a network of interconnected flexible polymer chains is deformed.<sup>1</sup> Viscoelastic rubbers are produced when a polymeric liquid is transformed into a contiguous network by tethering polymer chains together with covalent cross-links (“network junctions”). The concentration of junctions (the cross-link density) profoundly influences the mechanical properties of the network. And when the chain length between covalent junctions,  $M_x$ , exceeds the entanglement molar mass of the polymer chain,  $M_e$ , the more subtle influences of chain entanglements begin to dominate the viscoelasticity.<sup>2</sup> We recently introduced<sup>3</sup> a specially tailored nuclear magnetic resonance (NMR) spin echo function,  $\beta$ , that is inherently sensitive to the weak dipolar interactions among the protons and thereby capable of delineating slow, cooperative, multichain processes. Herein we quantitatively measure the residual dipolar interactions in poly(dimethylsiloxane) (PDMS) model networks prepared from carefully characterized, difunctional, PDMS precursor chains via “end-linking” chemistry using a tetrafunctional cross-linking agent. We examine the residual dipolar interactions as a function of the cross-link density and the amount of “pendent chain” defects—elastically ineffective chains having only one end attached to a junction—and interpret our findings in terms of models for network dynamics. NMR findings on networks are often characterized as exhibiting both liquidlike and solidlike features, features that could have been anticipated from early work on entangled melts.<sup>4,5</sup> Intuitive models of network dynamics<sup>6</sup> ascribed qualitatively different NMR characteristics to the “gel” (the covalently cross-linked 3-D network) and the “sol” (the unattached fragments

of polymer and, to varying degrees, the pendent defect chains in the network). Over the years, more detailed descriptions of network dynamics have emerged,<sup>7,8</sup> and more sophisticated NMR experiments and associated interpretations have targeted elastic networks.<sup>9–11</sup>

A microscopic understanding of network properties is very challenging as the delicate interplay between local mobility and long-range topological constraints is difficult to quantify. For example, local segmental motion is nearly isotropic, but there remains an inherent anisotropy which leads to nonzero averages of second-rank tensorial spin interactions that is readily apparent in NMR measurements sensitive to a hierarchy of dynamical processes. The origin of this anisotropy lies in a residual influence on segmental motion coming from the network topology. The weak residual dipolar interactions were used as a probe of slow polymer dynamics in PDMS melts recently.<sup>12</sup> We extend those measurements to PDMS networks. Unlike those used in previous studies of chain order and dynamics, these networks are particularly well characterized, having been made from precursor chains of known functionality and known molecular weight. Furthermore, the soluble fraction of these networks has been extracted and calculated in order to ascertain the fraction of chains contributing to network elasticity,  $f_{el}$ , and thereby the fraction of pendent “defect” chains which are dangling.<sup>2</sup> We have chosen to study this system using the  $\beta$ -echo (or sine correlation) NMR technique because the method is uniquely sensitive to dipolar interactions, and in particular, the degree to which the dipolar Hamiltonian can be regarded as static or fluctuating.

## Theory

**Dipolar Interactions and the Sine Correlation Experiment.** The experiments performed here utilize the secular dipolar term in the proton spin Hamiltonian

$$H_{D0}(t) = \frac{\mu_0 \gamma^2 \hbar}{4\pi r_{12}^3} P_2(\cos \theta(t)) [3I_1 z I_2 z - \mathbf{I}_1 \cdot \mathbf{I}_2] \quad (1)$$

<sup>†</sup> Massey University.

<sup>‡</sup> University of North Carolina at Chapel Hill.

\* Corresponding author.

where  $P_2(\cos \theta)$  is the second-order Legendre polynomial,  $1/2(3 \cos^2 \theta - 1)$  and where the polar angle  $\theta(t)$  describes the fluctuating orientations (with respect to  $z$ , the magnetic field direction) of the internuclear vector. The nuclear constants  $\mu_0$  and  $\gamma$  have their usual meaning, and  $h$  is Planck's constant. Note that the Hamiltonian of eq 1 applies to isolated pairs of spins separated by a distance  $r_{12}$ , an important point to which we shall return.

In this work we will be concerned both to probe the magnitude of the secular spin-pair dipolar interaction and to measure its fluctuations. The specific NMR approach used for this purpose will be the  $\beta$ -echo or "sine correlation" method. This technique has the advantage that all Zeeman terms in the spin Hamiltonian that are linear in the spin operators are refocused, so that the resulting NMR signal contains no modulations due to chemical shift or diamagnetic susceptibility effects. Furthermore, the very existence of the  $\beta$ -echo signal gives an indication of the dipolar interactions, since the signal is a null in the absence of bilinear spin operators in the Hamiltonian. A detailed analysis of this method has been given in earlier references, and only the salient points will be covered here. However, we will find it necessary to further develop the theoretical treatment of the interactions terms, as they specifically relate to polymer networks. In particular, we shall be concerned with dipolar interaction terms that remain stationary, reflecting the average local order in the network, as well as terms that fluctuate due to network dynamics.

Fluctuations in  $H_{D0}(t)$  cause a modulation in the dipolar precession frequencies,  $\omega_D(t)$ , and because of the stochastic nature of the processes associated with term  $P_2(\cos \theta(t))$ , we will find it convenient to describe  $\omega_D(t)$  in terms of the correlation function  $\langle \omega_D(t) \omega_D(0) \rangle$  and its initial value,  $\langle \omega_D(0)^2 \rangle$ , the second moment of the dipolar line shape,  $M_2$ . For a spin pair in the absence of motion, eq 1 gives<sup>13</sup>

$$M_2 = \frac{9}{20} \left( \frac{\mu_0 \gamma^2 \hbar}{4\pi} \right)^2 \frac{1}{r_{12}^6} \quad (2)$$

where  $r_{12}$  is the internuclear distance.

The  $\beta$ -echo NMR method can be used to measure quite small proton dipolar interactions by means of a pulse sequence which directly produces a dipolar sine correlation function without an influence from magnetic terms. The experiment generates a superposition of signals,  $[S_1 - S_2 - S_3]$  where  $S_1$ ,  $S_2$ , and  $S_3$  are the respective signals arising from  $(90^\circ_x - \tau - 90^\circ_y)$ ,  $(90^\circ_x - \tau - 90^\circ_x)$ , and  $(90^\circ_x - \tau - 180^\circ_y)$  spin-echo experiments, this superposition being created in a single-pulse sequence under appropriate phase-cycling conditions. The resulting normalized echo function,<sup>3</sup>  $\beta(\tau)$ , is independent of dephasing effects arising from magnetic inhomogeneity or chemical shifts, effects which would normally mask the dipolar interactions in conventional NMR spectroscopy and which prove extremely troublesome in other dipolar echo experiments. For this experiment the relevant spin-pair average is

$$\beta(\tau) = \langle \sin \phi(0, \tau) \sin \phi(\tau, 2\tau) \rangle \quad (3)$$

where the time  $t = 2\tau$  corresponds to the instant when the magnetic precessions are refocused in the spin echo. Equation 3 can be evaluated by making the Anderson-

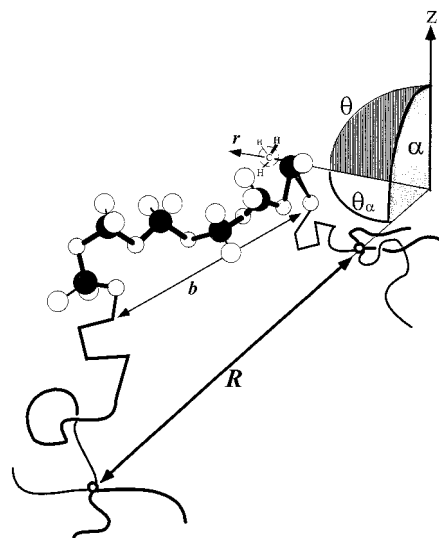


**Figure 1.** A schematic PDMS chain spanning two covalent cross-links is shown on several length scales. The (freely jointed) Kuhn segment  $b$  is comprised of approximately five PDMS monomers. On a longer length scale—between covalent junctions—the tethered (Gaussian) chain defines  $R$ , a director (along the end-to-end vector spanning two junctions) at orientation  $\alpha$  relative to the  $z$ -axis. In a rapidly rotating methyl group the proton dipolar interaction is determined by the instantaneous orientation of the  $C_3$  axis  $r$ .  $\theta$  is the polar angle between  $r$  and the magnetic field direction ( $z$ -axis);  $\theta$  can be defined in terms of the angles  $\alpha$  and  $\theta_\alpha$ , where the latter is the instantaneous orientation of  $r$  relative to  $R$ . The dipolar interaction is "preaveraged" along  $R$  by fast local motions—methyl group rotation, intra-Kuhn segment isomerization, and reorientations of  $b$  by (restricted) Rouse modes—to yield a residual proton second moment,  $\overline{M_2} = M_2 \langle \langle P_2(\cos \theta_\alpha(t)) \rangle \rangle_{\text{fast}}^2 \approx 10^5 \text{ s}^{-2}$ .

Weiss assumption<sup>14</sup> that the frequencies,  $\omega(t)$ , and phases,  $\phi(0, t) = \int_0^t \omega_D(t') dt'$ , are Gaussian distributed. Hence, it may be easily shown that

$$\langle \beta(\tau) \rangle = \exp(-\langle \phi(0, \tau)^2 \rangle) \sinh(\langle \phi(0, \tau) \phi(\tau, 2\tau) \rangle) \quad (4)$$

where

$$\langle \phi(0, \tau)^2 \rangle = 2 \int_0^\tau dt' (t - t') C(t') \quad (5)$$

and

$$\langle \phi(0, \tau) \phi(\tau, 2\tau) \rangle = \int_0^\tau dt' t' C(t) + \int_\tau^{2\tau} dt' (2\tau - t') C(t') \quad (6)$$

where  $C(t) = \langle \omega_D(t) \omega_D(0) \rangle$  is the correlation function.

**Static and Fluctuating Terms in Polymer Networks.** We now seek to evaluate the sine correlation function for the protons on polymer chains in a network. To see how this might be done, we need to consider how the network characteristics are expressed via eq 1. For a monomer of the polymer chain labeled by a proton spin pair the internuclear vector may be used to characterize the segment orientation by means of the polar angle  $\theta$  subtended with the axis of the polarizing magnetic field,  $B_0$ , as shown in Figure 1. The fluctuations in the dipolar precession frequency may then be expressed by considering fluctuations in  $\theta$ . For the polymer networks, in addition to local motions (methyl rotation and isomerizations), these motions may comprise the rapid segmental motion, as well as the slower excursions associated with whole chain reorientation.

In NMR analyses of Hamiltonian spin dynamics, it is often helpful to invoke the concept of motional hierarchy. Motional regimes may then be distinguished according to their rapidity vis-à-vis the characteristic time scale for the interaction strength, and in the present case the regimes are determined by comparison with the rigid lattice  $M_2^{-1/2}$ , of around  $10^{-6}$  s. We shall also be concerned with dipolar interactions on a polymer chain which are substantially but incompletely "pre-averaged" due to fast anisotropic internal motions. The residual second moment in this case will be referred to as  $\overline{M_2}$  and in this study will be found to give a characteristic time  $\overline{M_2}^{-1/2}$  of around  $10^{-3}$  s.

In the case of network dynamics, such a neat subdivision is not strictly possible. Consider the case of a chain of  $N$  monomers tethered at each end by a multifunctional cross-link to other chains. We would find it convenient to separate the internal segmental motions within the chain from the motion of the end-to-end vector of the chain associated with excursions at the end points ( $\mathbf{R}$  in Figure 1). However, segmental motions are governed by modes that encompass a wide range of time scales, right up to the terminal relaxation time of the chain, and this time will be comparable with the duration of end excursions. Having said that, we will nonetheless attempt such a hierarchical separation for the simple reason that it makes the theoretical treatment more tractable. We justify this by noting that, for most spins in the chain segments, the most rapid modes of the chain will dominate the motional averaging phenomenon. Furthermore, we note that NMR spin-locking measurements in polymer networks by Sotta et al.<sup>10</sup> indicate that the effective internal mode correlation times are shorter than  $10^{-4}$  s and thus much shorter than the characteristic time associated with the residual dipolar interaction as seen both in their own experiments and in our experiments reported here. This indicates that the influence of very slow modes of segmental reorientation is sufficiently weak that the motional hierarchy can be applied with some accuracy.

A much more complex issue concerns the use of the two-spin assumption which underpins the depiction of dipolar phase refocusing in the simple solid echo, ( $90^\circ_x - \tau - 90^\circ_y$ ). The dipolar-coupled methyl protons of PDMS, in rapid rotation around the  $C_3$  axis, yield total angular momentum eigenstates whose symmetries are equivalent to one spin  $3/2$  and two spin  $1/2$  systems<sup>15-17</sup> for which the dipolar splitting is only manifest in the  $3/2$  eigenstate. However, in PDMS, a second methyl group exists in close proximity so that further inter-methyl coupling results in a superposition of  $I = 0$  (5-fold),  $I = 1$  (9-fold),  $I = 2$  (5-fold), and  $I = 3$  (1-fold) total angular momentum states. For PDMS having freely rotating methyl groups with tetrahedral geometry and interproton distance  $r = 1.78$  Å, we find only a factor of 12 smaller (average) inter-methyl dipolar interaction ( $\langle r^3 \rangle = 68.8$  Å<sup>3</sup>) relative to the intra-methyl interaction ( $r^3 = 5.64$  Å<sup>3</sup>). The  $I = 0$  state is NMR invisible while all remaining states exhibit the dipolar splittings.

Only the  $I = 1$  states (i.e., those arising from single spin pair equivalents) experience perfect dipolar phase refocusing under a simple solid echo employed in the  $\beta$  pulse sequence. Through space dipolar interactions couple spins over all length scales. Hence, given sufficient interaction time, the phase evolution acquired by a single spin due to the dipolar coupling with its nearest neighbor will always be augmented by phase

evolution caused by interactions with successively more distant spins. Because the quantum mechanics that describes these evolutions involves unitary operators, it is possible in principle to completely reverse such dephasing, given a pulse sequence that can fully reverse the sign of the dipolar Hamiltonian. The solid echo does so for the two-spin dipolar interaction. For multiple spin contacts, the magic echo sequence,<sup>18</sup> involving a train of closely spaced rf pulses, is needed. Consequently, we expect that the  $\beta$  function which we generate using the solid echo will eventually suffer a decoherence which will cause it to decay. Sotta et al. used 2D-exchange spectroscopy to investigate the role of longer range dipolar interactions between other than neighboring spin pairs in polymer networks.<sup>10</sup> In particular, they found no observable magnetization transfer between CH<sub>2</sub> and CH protons in butadiene-based elastomers over the relevant time scale for the dipolar interaction, thus providing some support for the two-spin concept. However, we note that such an assumption is not required in most of our analysis and, in particular, is not necessary in analyzing the initial behavior of  $\beta$ . Hence, the residual dipolar second moments so obtained will be accurate. We do make implicit reference to the two-spin model in the simple theoretical treatment of the network dynamics but point out the role of higher-order interactions when necessary.

Suppose the internuclear vector  $\mathbf{R}$  makes an angle  $\theta_\alpha$  with respect to a second axis which in turn is inclined at  $\alpha$  to  $\mathbf{B}_0$ . We will take  $\alpha(t)$  to represent the inclination of the chain end-to-end vector with the magnetic field. Then the factor  $P_2(\cos \theta(t))$  in eq 1 can be decomposed into the product  $P_2(\cos \theta_\alpha(t))P_2(\cos \alpha(t))$ . If  $\theta_\alpha(t)$  fluctuates rapidly by comparison with  $M_2^{-1/2}$ , then the first Legendre polynomial can be replaced by its time-average,  $\overline{P_2(\cos \theta_\alpha(t))}$ ; the remaining angular dependence in eq 1 will derive entirely from the remaining fluctuations in  $\alpha(t)$ , and the effect of the fast motion is simply to rescale the strength of the dipolar interaction by  $\overline{P_2(\cos \theta_\alpha(t))}$ . The problem of what dipolar interaction remains following the segmental motions of a tethered chain has been addressed by a number of authors,<sup>7,19</sup> and it is found that for  $N$  Kuhn segments the dipolar reduction factor,  $\overline{P_2(\cos \theta_\alpha(t))}$ , is on the order of  $N^{-1}$ . More precisely, the degree of motional averaging will depend on the degree to which the chain is stretched. For an equilibrium mean-squared chain length of  $Nb^2$  ( $N$  Kuhn segments of length  $b$ ), let the instantaneous length in the network environment be  $R$ . Then the remaining dipolar rescaling factor becomes

$$\overline{P_2(\cos \theta_\alpha(t))} = \frac{3}{5} \frac{1}{N} \frac{R^2}{Nb^2} \quad (7)$$

Given an end-to-end vector  $\mathbf{R}(X, Y, Z)$ , and noting  $P_2(\cos \alpha) = 1/2(3Z^2 - R^2)/R^2$ , it may be seen that the overall orientation factor from eq 1 is given by

$$\overline{P_2(\cos \theta_\alpha(t))} P_2(\cos \alpha(t)) = \frac{3}{5} \frac{1}{N} \frac{2Z^2 - X^2 - Y^2}{2Nb^2} \quad (8)$$

It is well-known that the constraints to segmental motion in polymer networks arise not only from chemical cross-links but also from physical entanglements. In this paper we shall not distinguish these a priori as regards their influence in the dipolar interactions, but

rather we will seek to directly measure those interactions and then interpret them in terms of the known network parameters and known entanglement lengths for the poly(dimethylsiloxane) network precursor chains.

**A Simple Model for a Polymer Network Sine Correlation Function.** Protons in the polymer networks will be confined to chains that exist in some particular mean orientation and degree of extension but which undergo excursions from mean orientation and extension, due to slow network dynamics. Equation 8 can incorporate these motions by simply allowing that the  $\mathbf{R}$  vector ( $X, Y, Z$ ) is time-dependent with mean value ( $\bar{X}, \bar{Y}, \bar{Z}$ ). When the orientation factors of eq 1 are inserted into the expression for the dipolar Hamiltonian, the resulting expression may be separated into two parts: one with a time-zero average and one which represents the temporal mean, i.e.

$$H_{D0}(t) = \overline{H_{D0}} + (H_{D0}(t) - \overline{H_{D0}}) \quad (9)$$

We shall describe the dipolar precession frequencies deriving from these terms as

$$\omega_D(t) = \omega_D + \delta\omega_D(t) \quad (10)$$

Clearly, the mean vector determines the average dipolar frequency  $\omega_D$  while the excursions in [ $X(t), Y(t), Z(t)$ ] determine the values of  $\delta\omega_D(t)$ . The details of the relationships between  $\omega_D$  and  $\delta\omega_D(t)$  and their respective distributions over all possible chain lengths and orientations are subtle, making the issue of how to perform appropriate ensemble averages not at all straightforward. Furthermore, even if an appropriate model for the dynamics of the chain ends could be found, the basis of the dipolar interaction dependence on chain vectors as expressed in eq 8 is clearly inadequate, since it is based on a picture of phantom chains in which excluded-volume interactions play no role. It is known, for example, that this phantom chain model fails to reproduce the observed NMR spectra for polymer networks under extension.

Our approach to the treatment of the problem is to adopt a model for the chain dipolar interactions that is as simple as possible and that involves the minimum number of fitted parameters. We begin by considering a subensemble of spins confined to a family of chains whose end-to-end vectors are given by the coordinates ( $\bar{X}, \bar{Y}, \bar{Z}$ ). Having written down the NMR  $\beta$  signal for that subensemble, we then perform an average over all vectors ( $\bar{X}, \bar{Y}, \bar{Z}$ ). The averaging assumptions are as follows.

(i) The distribution on  $\delta\omega_D(t)$  is common to all subensembles.

(ii) An exponential correlation function is adopted for  $\delta\omega_D(t)$ .

(iii) In a given subensemble,  $\delta\omega_D(t)$  has a Gaussian distribution.

(iv) The distribution of static frequencies,  $\omega_D$ , over all subensembles, is taken to be Gaussian. We justify these assumptions in the following way.

(i) The angular excursions of the network junctions are taken to be large, encompassing a significant proportion of available solid angle. This is a reasonable picture, given that the excursion distance is expected to be on the order of the inter-cross-link chain length.<sup>20</sup> If large excursions are found, then their influence on

the dipolar interactions will be similar, irrespective of the mean orientation, ( $\bar{X}, \bar{Y}, \bar{Z}$ ).

(ii)–(iv) An exponential correlation function is the simplest way to describe the dynamics in terms of a single mode. The Gaussian assumptions are made for mathematical tractability. In support of (iv) we note that the distribution of static frequencies,  $\omega_D$ , is certainly smooth, as is apparent from a lack of oscillations in the observed  $\beta(\tau)$  functions or in the NMR free induction decays.

Writing

$$\begin{aligned} \phi(0, t) &= \omega_D t + \int_0^t dt' \delta\omega_D(t') \\ &= \omega_D t + \delta\phi(0, t) \end{aligned} \quad (11)$$

it may be easily shown that the subensemble average for the chain or for that family is given by

$$\begin{aligned} \langle \beta(\tau) \rangle_{XYZ} &= \sin^2(\omega_{DXYZ}\tau) \exp(-\langle \delta\phi(0, \tau)^2 \rangle) \times \\ &\quad \cosh(\langle \delta\phi(0, \tau) \delta\phi(\tau, 2\tau) \rangle) + \cos^2(\omega_{DXYZ}\tau) \times \\ &\quad \exp(-\langle \delta\phi(0, \tau)^2 \rangle) \sinh(\langle \delta\phi(0, \tau) \delta\phi(\tau, 2\tau) \rangle) \end{aligned} \quad (12)$$

The form of  $\beta(\tau)$  given in eq 12 has clear oscillatory character as a result of the static part of the interaction. Gaussian ensemble averaging on  $\omega_{DXYZ}$  results in

$$\begin{aligned} \langle \beta(\tau) \rangle &= \frac{1}{2} [1 - \exp(-2\langle \omega_D^2 \rangle \tau^2)] \exp(-\langle \delta\phi(0, \tau)^2 \rangle) \times \\ &\quad \cosh(\langle \delta\phi(0, \tau) \delta\phi(\tau, 2\tau) \rangle) + \\ &\quad \frac{1}{2} [1 + \exp(-2\langle \omega_D^2 \rangle \tau^2)] \exp(-\langle \delta\phi(0, \tau)^2 \rangle) \times \\ &\quad \sinh(\langle \delta\phi(0, \tau) \delta\phi(\tau, 2\tau) \rangle) \\ &= \exp(-\langle \delta\phi(0, \tau)^2 \rangle - \langle \omega_D^2 \rangle \tau^2) \sinh(\langle \delta\phi(0, \tau) \delta\phi(\tau, 2\tau) \rangle + \langle \omega_D^2 \rangle \tau^2) \end{aligned} \quad (13)$$

The quantity  $\langle \omega_D^2 \rangle$  is, by definition, the second moment of the spectrum generated by the residual dipolar couplings. We parametrize  $\langle \omega_D^2 \rangle$  and the correlation function for  $\delta\omega_D(t)$  by

$$\langle \omega_D^2 \rangle = x \overline{M_2}$$

$$\langle \delta\omega_D(t) \delta\omega_D(0) \rangle = (1 - x) \overline{M_2} \exp(-t/\tau_c) \quad (14)$$

Thus,  $\langle \beta(\tau) \rangle$  is characterized by three experimental parameters:  $\overline{M_2}$ ,  $x$ , and  $\tau_c$ .  $\overline{M_2}$  may be naively regarded as the total dipolar second moment, following internal segmental preaveraging, and in the absence of chain end excursions  $x$  gives a measure of the proportion of the total preaveraged second moment which is associated with the static part of the Hamiltonian. In that sense,  $(1 - x)$  gives a measure of the chain end excursions.

Inspection of eq 13 shows that, in the limit as  $\tau \rightarrow 0$ ,  $\langle \beta(\tau) \rangle$  reduces to  $\overline{M_2} \tau^2$ , independent of  $x$ . Thus, the influence of the dipolar interaction strength,  $\overline{M_2}$ , will be found in the initial rate of rise of the  $\beta$  function, while that of the fluctuations will be found in the subsequent decay. This lower time limit corresponds to the region where the pairwise dipolar interactions dominate so that the solid echo refocusing assumptions which underpin the  $\beta$  pulse sequence should be valid. At longer times, the higher-order spin interactions will result in

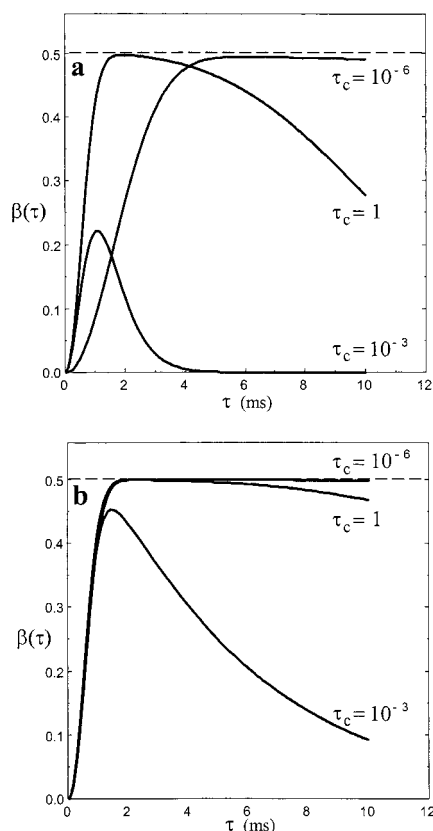


**Figure 2.** Plots of  $\beta(\tau)$  numerically evaluated from eqs 11–14 for a fixed value of  $\overline{M}_2 = 10^6 \text{ s}^{-2}$  and three values of  $\tau_c$  chosen to represent cases where  $\overline{M}_2^{1/2}\tau_c \gg 1$ ,  $\overline{M}_2^{1/2}\tau_c \sim 1$ , and  $\overline{M}_2^{1/2}\tau_c \ll 1$  for two values of  $x$ , where  $1 - x$  represents the chain end excursions; in Figure 1a,  $x = 0.1$ , and in Figure 1b,  $x = 0.9$ .

an additional decay so that the simple dynamical model discussed above may be inappropriate as decay caused by fluctuations may be dominated by  $T_2$ -like decay resulting from loss of coherence to nonrefocused higher-order dipolar effects. We are able to examine this effect by means of an experiment in which deuterons are used as the probe nucleus, since evolution under the  $I = 1$  quadrupole interaction will not be subject to these higher-order losses in coherence.

For purpose of the present exercise, we will find it useful to employ the simple exponential correlation function network excursion model, to parametrize the shape of the proton  $\beta$  curve, with the knowledge that representation of initial behavior will give correct values of the preaveraged dipolar interaction strength,  $\overline{M}_2$ . Figure 2a shows the form of the sine correlation function as given by eq 13 in which  $x$  is taken to be 0.1. Figure 2b shows a similar set, this time for  $x = 0.9$ . Three examples are shown in each figure, one with  $\overline{M}_2^{1/2}\tau_c \gg 1$ , one with  $\overline{M}_2^{1/2}\tau_c \sim 1$ , and one with  $\overline{M}_2^{1/2}\tau_c \ll 1$ . It is instructive to see how the parameters  $\overline{M}_2$ ,  $x$ , and  $\tau_c$  influence the shape of  $\beta(\tau)$ . For slow motion,  $\overline{M}_2^{1/2}\tau_c \gg 1$ , the initial rate of rise is determined by  $\overline{M}_2$ , and  $\beta(\tau)$  reaches a plateau value of 0.5. For rapid motion,  $\overline{M}_2^{1/2}\tau_c \ll 1$ , the initial rate of rise is determined by  $x\overline{M}_2$ , and again  $\beta(\tau)$  reaches a plateau value of 0.5. For intermediate motion,  $\overline{M}_2^{1/2}\tau_c \sim 1$ , the initial rate of rise is determined by  $\overline{M}_2$ , and  $\beta(\tau)$  reaches a

maximum value below 0.5, and which is determined by  $x$  and  $\tau_c$ , and then decays at a rate determined by  $\tau_c$ .

Now we are in a position to see how the influence of higher-order spin interactions will affect the process of parameter fitting. The reason that the  $\beta$  function rises to a plateau value of 0.5 is because of our assumption that the solid echo is capable of refocusing the precession due to the static part of the dipolar interaction. Once higher-order spin interactions introduce phase incoherence, this assumption breaks down. Consequently, we expect that at some time scale, longer than the NMR time scale  $\overline{M}_2^{-1/2}$  but related to that time, the  $\beta$  function will decay back to zero. This fact will impact directly on the fitting of  $\tau_c$ , in particular requiring us to return a value of  $\tau_c$  in the intermediate regime. A clue to this influence will be given by any observation that  $\tau_c$  appears closely related to the NMR time scale. Because of this ambiguity, we prefer to call our fitted  $\tau_c$  value an *apparent* correlation time.

## Experimental Section

Networks studied herein were synthesized from narrow MW distribution fractions of bifunctional poly(dimethylsiloxane) precursor chains comprised of vinyl-terminated PDMS having molar mass  $M_x$  ranging from 2460 to 58 000 Da (designated "B2" in ref 2) and a tetrafunctional cross-linking agent (tetrakisdimethylsilane) via platinum-catalyzed hydrosilylation chemistry for rheological studies in the laboratory of C. Cohen. Model networks (samples I–VI) were prepared by optimizing the ratio of cross-linking agent to precursor chains; model network VII was prepared from perdeuterated precursor PDMS. Two samples networks with enhanced dangling chain defects (III\* and III\*\*) were prepared by purposely adding monofunctional PDMS to preparations of (model) network III. The network characteristics (including original sample designations) are shown in Table 1.

NMR samples were prepared by placing into open-ended 2.5 mm diameter glass tubes a fragment of solid network with dimensions of 2–3 mm. The glass tube was then placed into a 3 mm i.d. solenoidal rf coil so that the sample was centrally positioned in the most homogeneous region of the rf field. Temperature control was achieved using an air stream that passed through a jacket surrounding the coil. A thermocouple placed in this stream close to the coil was used to regulate the temperature via standard feedback.

$^1\text{H}$  NMR experiments were carried out at 300 MHz using a Bruker AMX300 spectrometer and a 89 mm vertical bore superconducting magnet. The pulse sequence used to generate the  $\beta$ -echo signal is a composite one comprised of  $90^\circ$  and  $45^\circ$  rf pulses using a specialized phase cycling pattern, details of which can be found in ref 3. This cycle is completed in 24 separate steps, and this was the standard number of acquisitions used per delay time,  $\tau$ . It should be noted that the  $\beta$ -echo requires good rf homogeneity and accurate rf pulse durations in order to work well, and we have taken particular care before every measurement to optimize all pulse settings.

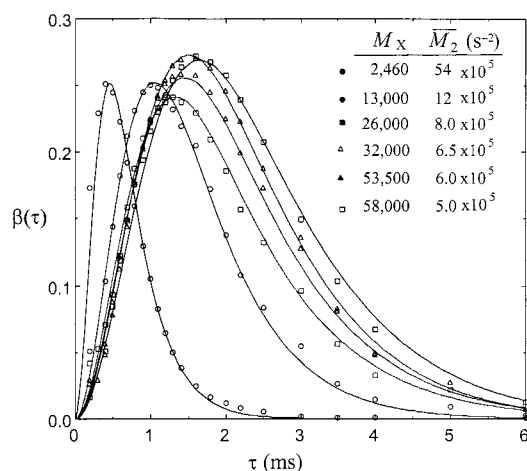
## Results

Figure 3 shows the sine correlation functions obtained from the set of model networks using proton NMR. Figure 4 contrasts the sine correlation functions for two nearly equivalent model networks: The proton  $\beta(\tau)$  for a PDMS network ( $M_x = 13\,000$  Da) is shown along with a deuterium NMR  $\beta(\tau)$  curve obtained by using a perdeuterated network ( $M_x = 19\,000$  Da). This latter  $\beta(\tau)$  curve has about the same rate of initial rise (i.e., the same interaction strength,  $\overline{M}_2 = 2 \times 10^6 \text{ s}^{-2}$ ) as the proton  $\beta(\tau)$  curves from the networks formed comparable precursor chains. However, it is immediately apparent that the rate of decay of the deuterium  $\beta(\tau)$  function is

Table 1. Characteristics of PDMS (Model) Network Samples

PDMS networks	precursor chain length $M_X$ (Da)	weight fraction of elastic chains $f_{el}$	residual second moment $\overline{M}_2$ ( $s^{-2}$ )	magnitude of apparent chain-end excursion parameter $x$	apparent correlation time $\tau_c$ (ms)
<b>I</b> {A-1} <sup>a</sup>	2 460	0.87	5 400 000	0.40	0.35
<b>II</b> {C-1} <sup>b</sup>	13 000	0.85	1 200 000	0.38	0.90
<b>III</b> {C-1} <sup>c</sup>	26 000	0.80	800 000	0.38	0.90
III* {C-2} <sup>c</sup>	26 000	0.48			
III {C-3} <sup>c</sup>	26 000	0.24			
<b>IV</b> {C-3} <sup>b</sup>	32 000	0.81	650 000	0.40	1.20
<b>V</b> {A-III} <sup>a</sup>	53 500	0.90	600 000	0.43	1.50
<b>VI</b> {A-12} <sup>a</sup>	58 000	0.72	500 000	0.42	1.60
<b>VII</b> {A-1} <sup>c</sup>	19 000	0.86	2 000 000		

<sup>a</sup> Patel, S.; Malone, S.; Cohen, C.; Gillmor, J.; Colby, R. *Macromolecules* **1992**, *25*, 5421. <sup>b</sup> McLoughlin, K.; Waldbieser, J. K.; Cohen, C.; Duncan, T. M. *Macromolecules* **1997**, *30*, 1044. <sup>c</sup> McLoughlin, K.; Szeto, C.; Duncan, T. M.; Cohen, C. *Macromolecules* **1996**, *29*, 5475. Boldface designates model networks; **III** was diluted with monofunctional "defect" chains ( $M = 29\,000$  Da) to give III\* and III\*\*; { } is the original sample designation; **VII** is a perdeuterated PDMS model network.



**Figure 3.** Plots of  $\beta(\tau)$  for proton NMR of PDMS model networks for precursor chain molar masses ranging from  $M_X = 2460$  to  $M_X = 58\,000$  Da (see boldface sample entries in Table 1). The solid lines are calculated (see text), and the observed residual second moments from the initial slopes of the  $\beta(\tau)$  curves range from  $54 \times 10^5$  to  $5.0 \times 10^5$   $s^{-2}$ , respectively.

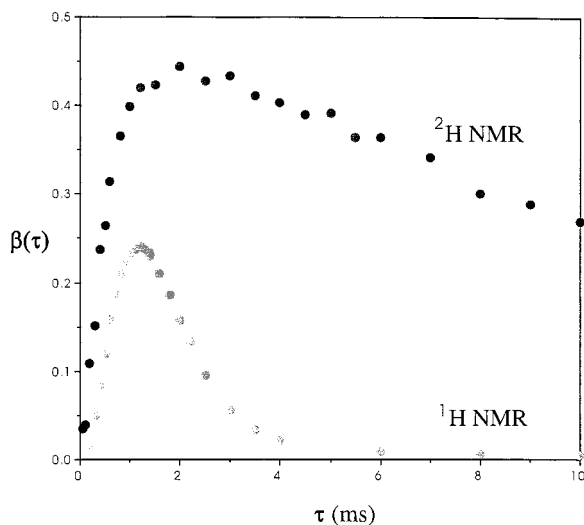


**Figure 4.** Plots of  $\beta(\tau)$  for deuterium and proton NMR of PDMS model networks **II** and **VII** having precursor chain molar masses  $M_X = 13\,000$  and  $19\,000$  Da, respectively.

much slower than that exhibited by the protons. This suggests that higher-order spin interactions are indeed playing a role in the proton experiments, so that the fitting of these data using the simple exponential correlation function network excursion model must be

considered an exercise in parametrization in which only the preaveraged dipolar interaction strength,  $\overline{M}_2$ , has real physical significance.

The proton data in Figure 3 have been fitted for  $\overline{M}_2$ ,  $x$ , and  $\tau_c$  using eq 11. In each case, we have allowed for the small ( $\sim 15\%$ ) fraction of dangling chains (see Table 1) by presuming that spins on these chains had their dipolar interactions entirely motionally averaged. Note that  $\beta(\tau)$  is calculated by taking the residual signal generated by dipolar interactions [ $S_1 - S_2 - S_3$ ] and then normalizing by the total NMR signal at  $\tau = 0$ , so that the effect of spin populations that do not experience dipolar interactions is to scale down the amplitude of the remaining  $\beta(\tau)$  in the normalization process. Consequently, the adjustment for dangling chains requires us to scale the theoretical  $\beta(\tau)$  by 85%, the mean elastic fraction for the model networks. However, we note that where no such adjustments are made the resulting parameter fits are still broadly consistent with those presented here, the major difference being in the size of the apparent excursion parameter,  $x$ .

In Figure 3 the fits are shown as solid lines, the resulting parameters being given in Table 1. Some obvious factors emerge when one considers the dependence of these parameters on the precursor chain length,  $M_X$ . First, the most dramatic influence of  $M_X$  is felt in the effective dipolar second moment,  $\overline{M}_2$ . Second, the apparent excursion parameter  $x$  is independent of  $M_X$ . Finally, the apparent correlation time,  $\tau_c$ , depends weakly on  $M_X$  and is on the order of 1 ms. This value is particularly significant because it does indeed correspond to the "NMR time scale scale"  $\overline{M}_2^{-1/2}$  and reinforces our interpretation that both this parameter and the apparent excursion parameter  $x$  are required to reproduce the observed shape of  $\beta(\tau)$  because of the inherent weaknesses in the simplistic two-spin assumption. By contrast, we attach real physical significance to the fitted  $\overline{M}_2$  parameter, which is obtained independently of the assumed dynamical model, since the initial behavior of  $\beta(\tau)$  is always of the form  $\overline{M}_2\tau^2$ .

We have also carried out sine correlation measurements on networks for which there have been deliberately incorporated, additional dangling chains. The experimental  $\beta(\tau)$  curves are shown in Figure 5. We have not attempted to fit these data using our analytic model because we believe that the rather simple assumptions, which might be justified when the proportion of dangling chains is small, are more questionable when these chains constitute the majority of the polymer segments. Certainly, a cursory examination of Figure 5 suggests

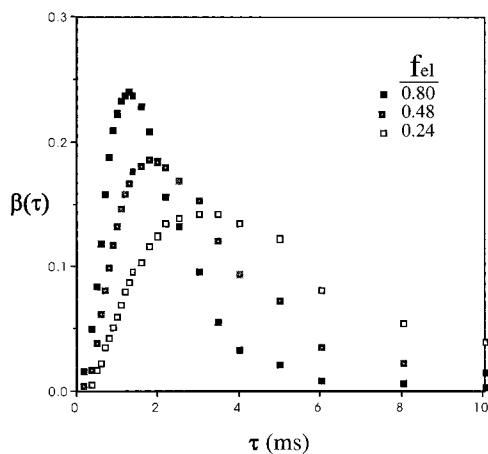


**Figure 5.** Plots of  $\beta(\tau)$  for proton NMR of a PDMS model network III with  $M_X = 26\,000$  Da and a fraction of elastically effective chains  $f_{el} = 0.80$ ; the model network is diluted with elastically ineffective chains by including monofunctional precursor chains ( $M = 29\,000$ ) prior to network formation yielding networks with  $f_{el} = 0.48$  (III\*) and  $f_{el} = 0.24$  (III\*\*).

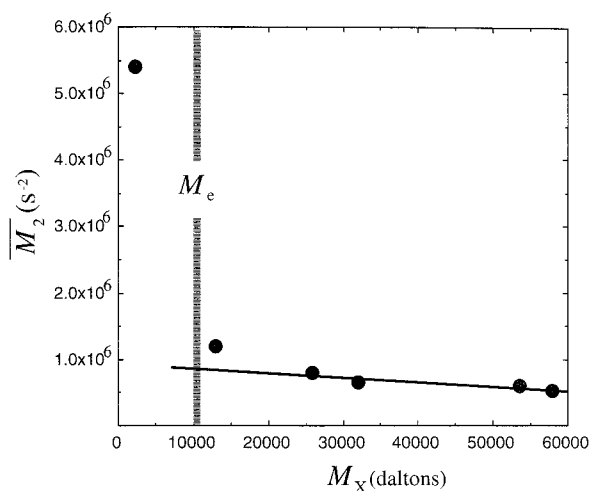


**Figure 6.** Observed residual second moment  $\overline{M}_2$  for model networks is shown versus network precursor chain length  $M_X$ .

that the effective second moments for these defective networks (III\* and III\*\*) are lower than those of the model network III.

## Discussion

Figure 6 shows the dependence of  $\overline{M}_2$  on the molar mass of the precursor chain,  $M_X$ . The apparent  $x$  and  $\tau_c$  values are shown in Table 1. The variation in the second moment is particularly instructive. In particular, we see that for precursor chain lengths below  $M_e \sim 10\,000$  Da the second moment exhibits a strong molar mass dependence. This strong dependence is exactly what we would expect given the chain length dependence of segmental motion preaveraging, namely  $P_2(\cos\theta_\alpha(t)) \sim N^{-1}$ . Above  $M_e$ , the  $\overline{M}_2$  data strongly inflect to a plateaulike behavior, in which only a weak molar mass dependence is observed. We interpret this effect as arising from the onset of physical entanglements once the precursor chain length exceeds the critical molar mass. However, the effect of chemical cross-links in restricting motional averaging has not entirely disappeared, as is clear from the significantly weaker but nonetheless observable decline in  $\overline{M}_2$  for  $M_X > M_e$ .

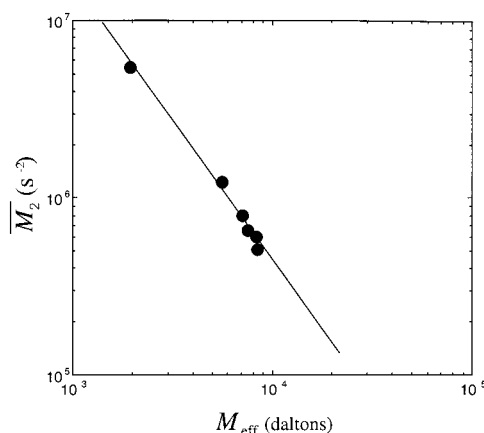


**Figure 7.** A log-log plot of the observed residual second moment  $\overline{M}_2$  for model networks versus network effective chain length  $M_{eff}^{-1} = M_X^{-1} + M_e^{-1}$ .

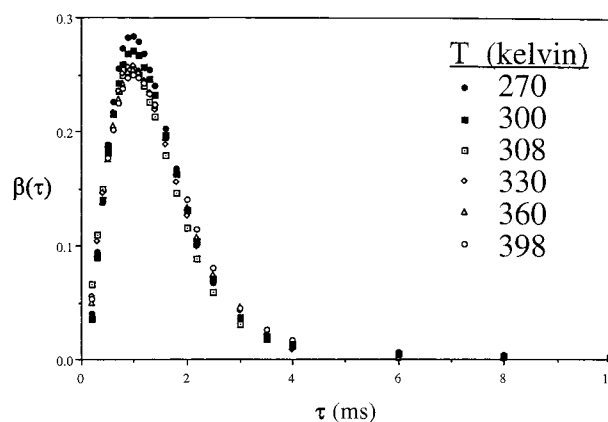


**Figure 8.** Temperature dependence of the proton  $\beta(\tau)$  of a PDMS model network II with  $M_X = 13\,000$  Da.

In the article by Sotta et al., a variety of styrene-butadiene rubbers are investigated using NMR  $T_2$  decays, and for these samples the inter-cross-link molar mass was always in excess of  $M_e$ . These authors argued that the effect of chemical cross-links and physical cross-links (entanglements) were additive as regards the residual dipolar interaction associated with  $P_2(\cos\theta_\alpha(t))$ . Consequently, they proposed a rule that the effective number of monomers sensed using NMR measurements of dipolar interactions was given by  $N_{eff}^{-1} = N_X^{-1} + N_e^{-1}$ . Following this reasoning, we have plotted our dipolar second moments against  $M_{eff}$  as shown in Figure 7. The data appear to follow a scaling relation of the form  $\overline{M}_2 \sim N_{eff}^{-1.6}$ , close to the  $N^{-2}$  scaling expected, given  $P_2(\cos\theta_\alpha(t)) \sim N^{-1}$ .

As indicated in the Theory section, the observed shape of the  $\beta$  function requires an apparent correlation time fortuitously comparable with the "NMR time scale",  $\overline{M}_2^{-1/2}$ , if we are to believe our simple model. This fortuitous effect arises because the value of  $\tau_c$  required is indicative of higher-order spin interactions whose dipolar precessions are unfocused in our experiment. Further support for that interpretation is found in another experiment in which we varied the temperature of the  $M_X = 13\,400$  network over a wide range from 270 to 380 °C. The results are shown in Figure 8.

Remarkably, the  $\beta(\tau)$  function is practically invariant on change of temperature, in marked contrast to the case of polymer melts, where increasing the tempera-

ture led to a motional averaging of the dipolar interactions and a collapse of the  $\beta(\tau)$  function to much smaller values.<sup>12</sup> Note that in the case of melts, where power law correlation functions govern the reptation dynamics, the Rouse times appear in the correlation function prefactor, which in turn governs the initial rate of rise of  $\beta(\tau)$  while the tube disengagement process leads to a total correlation loss and a decay of the height of  $\beta(\tau)$ . In networks, there is no terminal correlation loss, and no such power law dynamics are apparent so that the correlation function prefactor which governs the initial rate of rise of  $\beta(\tau)$  is determined entirely by  $\overline{M}_2$ . Consequently, we may understand why the initial rate of rise of the observed  $\beta(\tau)$  is temperature-independent. The significant anomaly is the lack of temperature dependence in long time behavior of  $\beta(\tau)$ , where network dynamics might be expected to be manifest. While it is of course possible that the network dynamics are only weakly dependent on temperature because of a particularly low activation energy for cross-link migration, we regard the interpretation of the apparent correlation times observed in our work as reflecting properties of the network spin couplings rather than the network motion. It is our intention to explore new versions of the  $\beta(\tau)$  sine correlation experiment in which more complete refocusing is achieved by means of multiple pulse coherent averaging methods.<sup>18</sup>

We note that Brereton<sup>21</sup> has developed a Gaussian chain network model which takes into account network fluctuations in a manner similar to that employed in our approach, namely by means of a simple exponential correlation function characterized by an excursion parameter and a correlation time. Brereton's model is more sophisticated than ours, in that it accounts for the full distribution of chain end-to-end vectors. However, this model predicts a similar  $\beta$ -echo shape to that obtained using the simpler model employed in this paper. And it suffers from the same difficulty, namely that it cannot account for the temperature independence of the shape of  $\beta(\tau)$  and cannot account for the difference in the shape of  $\beta(\tau)$  when measured using deuteron and proton NMR. If the decay of the proton  $\beta(\tau)$  is predominantly influenced by  $T_2$  effects arising from higher-order dipolar couplings, rather than by the network dynamics, then the only physically significant parameter that we are able to fit is the residual second moment  $\overline{M}_2$ , a quantity whose value is associated with the initial behavior of  $\beta(\tau)$  and which is not significantly perturbed by  $T_2$ . Such a fit is independent of the chosen dynamical model, and so we feel justified in using the simple picture employed herein.

## Conclusions

The  $\beta$ -echo or sine correlation method has been shown to produce results in poly(dimethylsiloxane) networks which are significantly different than in the case of poly(dimethylsiloxane) melts. We find clear evidence for nonzero anisotropic dipolar interactions which are particularly sensitive to the chain length,  $M_X$ , between cross-links. The strong dependence of the dipolar second moment on  $M_X$  for  $M_X < M_e$  is consistent with the concept of preaveraging within a chain fixed at each end

or, alternatively, a chain with virtual end chains fixed to points, as in the network fluctuation model of Rubinstein and Panyukov.<sup>20</sup> As  $M_X$  exceeds  $M_e$ , the dependence of the dipolar second moment dramatically changes, as physical entanglements begin to dominate the motional constraints. When both physical and chemical constraints are accounted for via an effective chain length  $M_{X\text{eff}}$ , then it is found that  $\overline{M}_2 \sim M_{X\text{eff}}^{-1.6}$ , consistent with the established model,  $\omega_d \sim N^{-1}$ .<sup>19</sup>

The network dynamics may be apparent in the data presented here, but it is more likely that these are masked by decoherence effects caused by higher-order spin interactions.<sup>22</sup> We propose to investigate these effects in future work, in particular by applying a new version of the  $\beta$  rf pulse sequence which more effectively refocuses dephasing caused by multiple spin interaction terms in the dipolar Hamiltonian.

**Acknowledgment.** We are indebted to Claude Cohen for many conversations during the course of this work and to his research group for the synthesis and characterization of the PDMS networks. We also thank Michael Rubinstein and Alexander Deshkovski for discussions of the analysis. E.T.S. acknowledges support from the National Science Foundation (DMR-9412701) and the John Simon Guggenheim Foundation; P.T.C. acknowledges support from the New Zealand Foundation for Research, Science and Technology and the Royal Society of New Zealand Marsden Fund.

## References and Notes

- (1) Treloar, L. A. G. *The Physics of Rubber Elasticity*, 2nd ed.; Oxford University Press: London, 1958.
- (2) Patel, S. K.; Malone, S.; Cohen, C.; Gillmor, J. R.; Colby, R. H. *Macromolecules* **1992**, *25*, 4241.
- (3) Callaghan, P. T.; Samulski, E. T. *Macromolecules* **1997**, *30*, 113.
- (4) Powels, J. G.; Hartland, A. *Nature* **1960**, *168*, 26.
- (5) McCall, D. W.; Douglass, D. C.; Anderson, E. W. *J. Polym. Sci.* **1962**, *59*, 301.
- (6) Folland, R.; Charlesby, A. *Polymer* **1979**, *207*, 207.
- (7) Cohen-Addad, J.-P. *Prog. NMR Spectrosc.* **1993**, *25*, 1 and references therein.
- (8) Brereton, M. G. *Macromolecules* **1993**, *23*, 1119.
- (9) Weber, H. W.; Kimmich, R. *Macromolecules* **1993**, *26*, 2597.
- (10) Sotta, P.; Fulber, C.; Demco, D. E.; Blumich, B.; Spiess, H. W. *Macromolecules* **1996**, *29*, 6222.
- (11) Fischer, E.; Grinberg, F.; Kimmich, R.; Hafner, S. *J. Chem. Phys.* **1998**, *109*, 846.
- (12) Callaghan, P. T.; Samulski, E. T. *Macromolecules* **1998**, *31*, 3693.
- (13) Abragam, A. *The Principles of Nuclear Magnetism*; Oxford University Press: Oxford, 1961.
- (14) Anderson, P. W.; Weiss, P. R. *Rev. Mod. Phys.* **1953**, *25*, 269.
- (15) Cohen-Addad, J.-P.; DuPeyre, R. *Polymer* **1983**, *24*, 400.
- (16) Andrew, E. R.; Bersohn, R. *J. Chem. Phys.* **1950**, *18*, 159.
- (17) Cobb, T. B.; Johnson, C. S. *J. Chem. Phys.* **1970**, *52*, 6224.
- (18) Rhim, W.-K.; Elleman, D. D.; Vaughan, R. W. *J. Chem. Phys.* **1973**, *59*, 3740. The use of "magic echoes" to delineate spin correlations in rubbers was explicitly suggested by G. Fink et al., Berlin AMPERE/ISMAR Conference Abstracts p 710, 1998.
- (19) Sotta, P.; Deloche, B. *Macromolecules* **1990**, *23*, 1999.
- (20) Rubinstein, M.; Panyukov, S. *Macromolecules* **1997**, *25*, 8036.
- (21) Brereton, M. G., private communication.
- (22) Gasper, L.; Demco, D. E.; Blumich, B. *Solid State Nucl. Magn. Reson.* **1999**, *14*, 105.